CrossMark

CHEST

CT and histopathologic characteristics of lung adenocarcinoma with pure ground-glass nodules 10 mm or less in diameter

Fang Wu[1,2] · Shu-ping Tian[3] · Xin Jin[1] · Rui Jing[1] · Yue-qing Yang[1] · Mei Jin[1] · Shao-hong Zhao[1]

Abstract

Objective To evaluate CT and histopathologic features of lung adenocarcinoma with pure ground-glass nodule (pGGN) ≤10 mm in diameter.

Methods CT appearances of 148 patients (150 lesions) who underwent curative resection of lung adenocarcinoma with pGGN ≤10 mm (25 atypical adenomatous hyperplasias, 42 adenocarcinoma in situs, 38 minimally invasive adenocarcinomas, and 45 invasive pulmonary adenocarcinomas) were analyzed for lesion size, density, bubble-like sign, air bronchogram, vessel changes, margin, and tumour-lung interface. CT characteristics were compared among different histopathologic subtypes. Univariate and multivariate analysis were used to assess the relationship between CT characteristics of pGGN and lesion invasiveness, respectively.

Results There were statistically significant differences among histopathologic subtypes in lesion size, vessel changes, and tumour-lung interface ($P<0.05$). Univariate analysis revealed significant differences of vessel changes, margin and tumour-lung interface between preinvasive and invasive lesions ($P<0.05$). Logistic regression analysis showed that the vessel changes, unsmooth margin and clear tumour-lung interface were significant predictive factors for lesion invasiveness, with odds ratios (95% CI) of 2.57 (1.17-5.62), 1.83 (1.25-2.68) and 4.25 (1.78-10.14), respectively.

Conclusion Invasive lesions are found in 55.3% of subcentimeter pGGNs in our cohort. Vessel changes, unsmooth margin, and clear lung-tumour interface may indicate the invasiveness of lung adenocarcinoma with subcentimeter pGGN.

Key points
• *Invasive lesions were found in 55.3% of lung adenocarcinomas with subcentimeter pGGNs*
• *Lesion size, vessel changes, and tumour-lung interface showed different among histopathologic subtypes*
• *Vessel changes, unsmooth margin and clear tumour-lung interface were predictors for lesion invasiveness*

Abbreviations

CT	Computed tomography
pGGN	Pure ground-glass nodule
AAH	Atypical adenomatous hyperplasia
AIS	Adenocarcinoma in situ
MIA	Minimally invasive adenocarcinoma
IPA	Invasive pulmonary adenocarcinoma
HU	Hounsfield unit
ANOVA	One-way analysis of variance
SNK	Student-Newman-Keuls
IASLC	International Association for the Study of Lung Cancer
ATS	American Thoracic Society
ERS	European Respiratory Society

Fang Wu and Shu-ping Tian contributed equally to this work.

✉ Shao-hong Zhao
zhaoshaohong@aliyun.com

1 Department of Radiology, Chinese PLA General Hospital, 28 Fuxing Road, Beijing 100853, China

2 Department of Radiology, Xuanwu Hospital, Capital Medical University, 45 Changchun Street, Beijing 100053, China

3 Department of Radiology, Navy General Hospital, 28 Fucheng Road, Beijing 100048, China

Introduction

With the popularization of low-dose computed tomography (CT) screening for lung cancer, pure ground-glass nodules (pGGNs) are increasingly detected [1]. Persistent pGGNs for more than 3 months correspond to atypical adenomatous hyperplasia (AAH), adenocarcinoma in situ (AIS) or invasive adenocarcinoma [2]. In addition, previous literature [3, 4] reported that prognosis for lung adenocarcinoma probably depended on the size of the invasive component. So it is very important to distinguish the invasiveness of those pGGNs for appropriate management. Air bronchogram, higher density or larger lesion size can indicate the malignancy of pGGNs [5–7]. A 10 mm diameter is used as a cutoff value to distinguish preinvasive and invasive lesions [8, 9]. However, some pGGNs ≤10 mm may be minimally invasive adenocarcinoma (MIA) or invasive pulmonary adenocarcinoma (IPA) [10–13]. Controversy and uncertainty remain regarding the management of pGGNs ≤10 mm. The correlation between CT characteristics and histopathologic subtypes of lung adenocarcinoma with pGGN ≤10 mm in diameter are not described clearly, and the decision for either follow-up or resection is a dilemma for both doctors and patients.

In this study, we aimed to clarify the CT features of lung adenocarcinoma with pGGN ≤10 mm in different histopathologic subtypes.

Materials and methods

This retrospective study was approved by the institutional review board of Chinese PLA General Hospital, which waived the requirement for patients' informed consent for the use of CT scanning

Patients

From March 2011 to February 2016, a total of 7352 consecutive patients who underwent curative resection of lung adenocarcinoma in our hospital were reviewed via the electronic medical records and the radiology information systems. Our inclusion criteria were as follows: (1) the presence of chest CT scan with thin-slice thickness (1–1.5 mm) within one week prior to surgery, (2) lesions showed pure ground-glass opacity on lung window images (level, −600 Hounsfield unit [HU]; width, 1500 HU), and (3) pGGNs ≤10 mm in the longest diameter on axial images. One hundred of sixty-five patients with lung adenocarcinoma showed pGGN ≤10 mm. Seventeen patients were excluded from the analysis, including nine patients without chest CT scan within one week prior to surgery, and eight patients without thin-slice CT images. A total of 148 patients (150 lesions) met the inclusion criteria. Pure GGNs disappeared or decreased in size on follow-up CT at 3 months were considered as infectious diseases. These nodules were surgically removed in our hospital depending on the size, the growth of pGGN and patients' decision. As for the

multiple nodules, the dominant nodule(s) and the nodules in the same lobe or side were usually selected for surgical resection. In our sample, two patients who had two pGGNs ≤10 mm located in the same lung lobe underwent resection simultaneously.

CT examinations

Chest CT was performed using the following scanners: Siemens Cardiac 64, and Philips Brilliance 256 iCT with 120 kVp, 100–200 mAs and a slice thickness of 5 mm. Then for contrast-enhanced CT scan, a bolus of 60 ml of nonionic iodinated (300 mg iodine per milliliter) contrast material (iopromidum, Ultravist 300; Bayer Schering Pharma, Berlin, Germany) was injected in an antecubital vein at a flow rate of 2.0-3.5 ml/s with a power injector (Stellant; Medrad, Indianola, PA, USA). Then image acquisition started 20–23 seconds after injection was finished. Images were reconstructed by using a medium sharp reconstruction algorithm with a thickness of 1–1.5 mm. CT scans were obtained in the supine position at full inspiration.

CT and histopathologic features analysis

Two experienced radiologists with more than ten years of experience in chest CT diagnosis who were blinded to the histopathologic results and clinical data independently evaluated the CT images. When the opinions of the two radiologists were divergent, the discrepancies were resolved by consensus. A pGGN was defined as purely of ground-glass opacity on lung window images (level, −600 HU; width, 1500 HU) that had no soft-tissue attenuation within the lesion on the mediastinal window images (level, 40 HU; width, 400 HU). Each lesion was assessed with a fixed lung window setting (level, −600 HU; width, 1500 HU) in terms of lesion size, mean CT attenuation, bubble-like sign, air bronchogram, vessel changes, margin, and tumour-lung interface. The lesion size was the maximal diameter (mm) on axial images. The mean CT attenuation (HU) was measured by placing a region of interest (ROI) of 8 mm^2 in three different sites within the nodule barring the vessels and bronchioles. Bubble-like sign was depicted as air attenuation vesicle-like lucency within the nodule. Vessel changes were defined as dilated/distorted vessels, and vascular convergence seen within GGNs. The margin was described as smooth, lobular, spiculated, and lobular with spiculated. A lobular margin was defined when a portion of the lesion's surface showed a wavy or scalloped configuration. A spiculated margin was defined as the presence of strands extending from the nodule margin into the lung parenchyma without reaching the pleural surface. Tumour-lung interface was recorded as clear if the nodules were well-defined.

One experienced chest pathologist reviewed the pathologic specimens. According to the 2015 World Health Organization classification of lung tumours, all lesions were classified into preinvasive lesions (AAH and AIS) and invasive lesions (MIA and IPA). Preinvasive lesions showed proliferation of mild to moderate cell
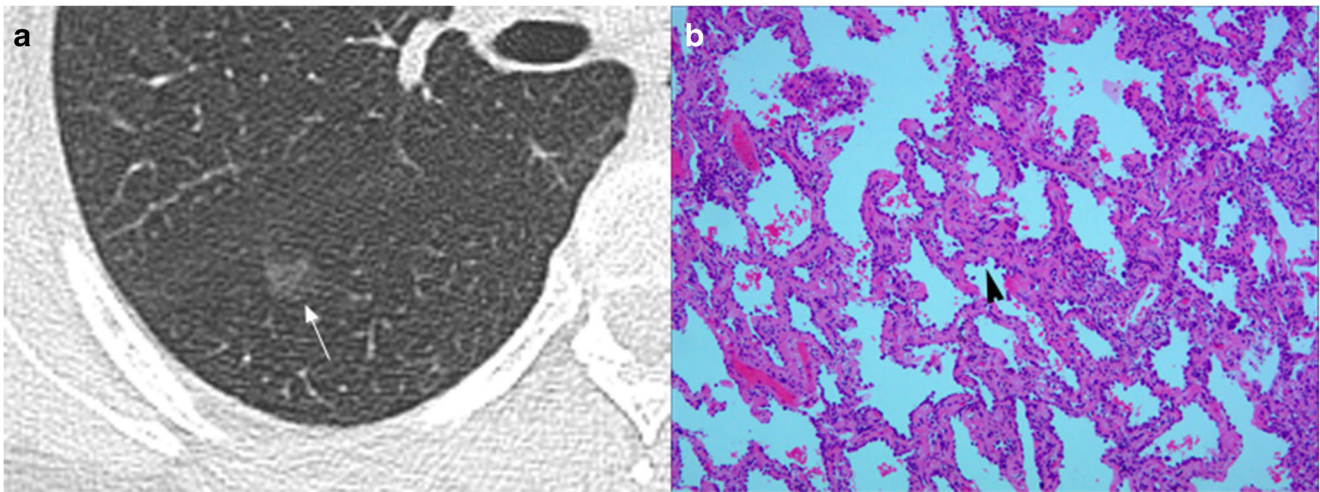
Fig. 1 CT and histopathologic photomicrograph of AAH **a**. Thin-section CT image shows a pGGN located in the superior segment of the right lower lobe (white arrow) with diameter of 9 mm, and unclear tumour-lung interface; **b**. Photomicrograph of histopathologic specimen shows atypical pneumocytes lining alveolar walls (black arrow) (Hematoxylin-eosin stain; original magnification, ×100)

atypia in type II pneumocytes and/or Clara cells or a small neoplasia with pure lepidic growth, along preexisting alveolar structures without stromal, vascular, or pleural invasion. While invasive lesions showed at least one focus of invasive adenocarcinoma.

Statistical analysis

All quantitative data were presented as mean ± standard deviation. Lesion size and density were compared among histopathologic subtypes using one-way analysis of variance (ANOVA) followed by the Student-Newman-Keuls (SNK) posttest. Lesion size and density were compared between preinvasive and invasive groups by 2-independent samples t test. Bubble-like sign, air bronchogram, vessel changes, margin, and tumour-lung interface were compared using Chi-square test. Logistic regression analysis with the method of forward stepwise (likelihood ratio) was used to assess the relationship between CT characteristics of pGGN and lesion invasiveness. A P-value less than 0.05 was considered statistically significant. All statistical analyzes were performed by using commercially available software (SPSS 22.0, IBM).

Results

### Patient demographics and histopathological diagnosis

Of the 150 lung adenocarcinomas, there were 25 AAHs (16.7%), 42 AISs (28.0%), 38 MIAs (25.3%) and 45 IPAs
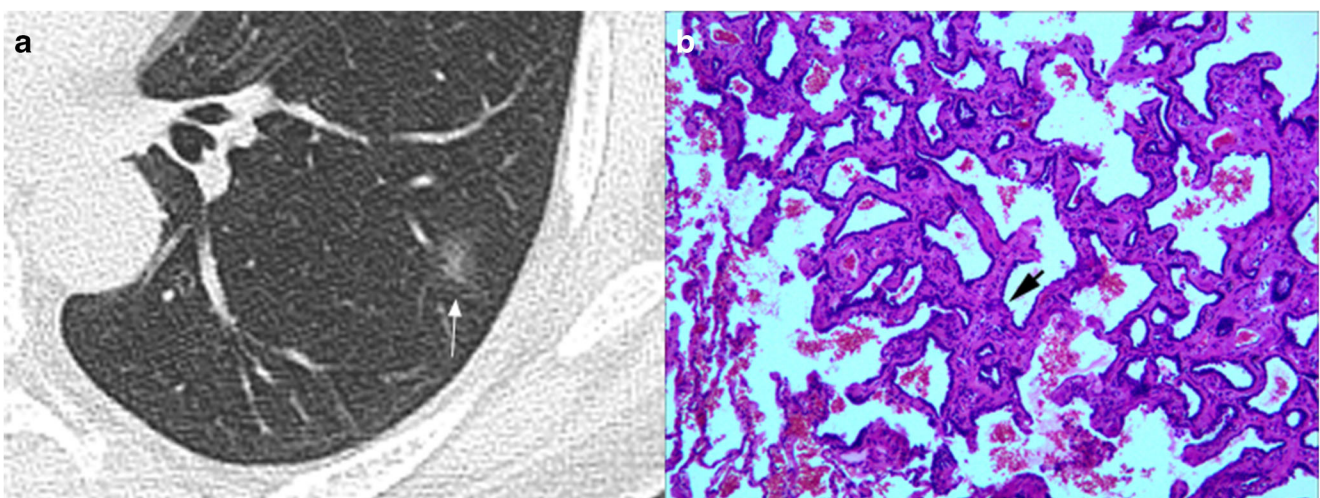
Fig. 2 CT and histopathologic photomicrograph of AIS **a**. Thin-section CT image shows a pGGN located in the lateral basal segment of the left lower lobe (white arrow) with diameter of 8 mm, nonuniform density and unclear tumour-lung interface; **b**. Photomicrograph of histopathologic specimen shows neoplastic cells lining preexisting alveolar structures without stromal, vascular, or pleural invasion (black arrow) (Hematoxylin-eosin stain; original magnification, ×100)
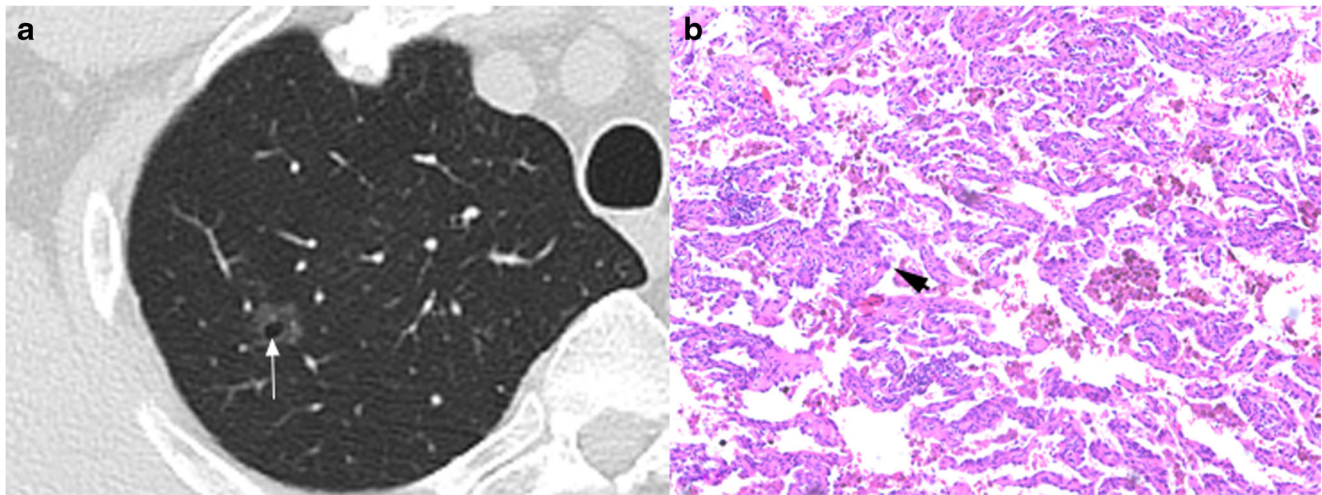
Fig. 3 CT and histopathologic photomicrograph of MIA **a**. Thin-section CT image shows a pGGN located in the apical segment of the right upper lobe with diameter of 9 mm, bubble-like sign inside the nodule (white arrow), slightly lobular margin, and clear tumour-lung interface; **b**.
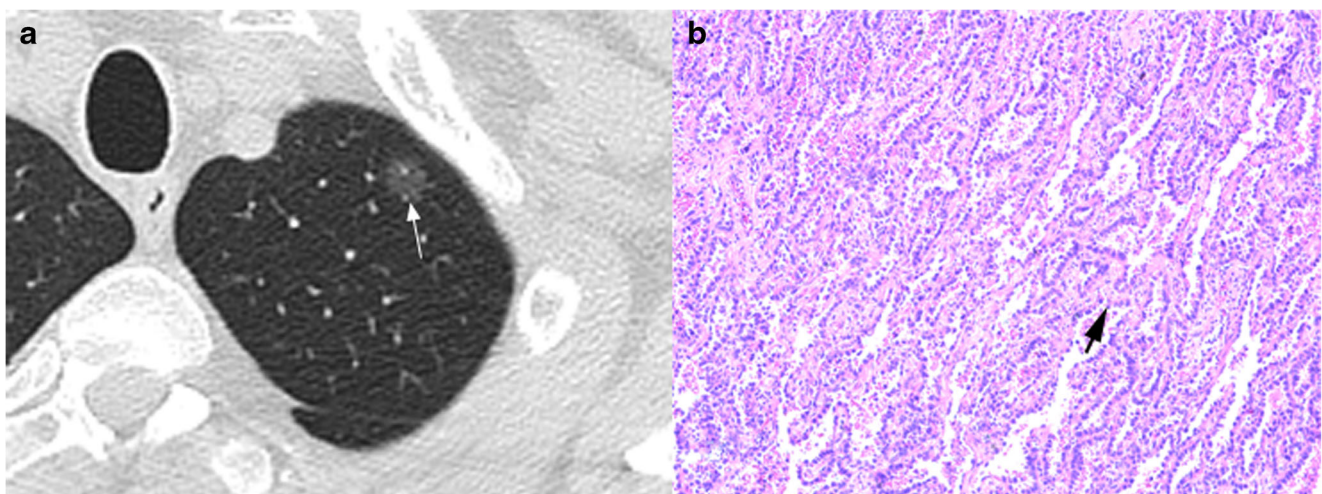
Photomicrograph of histopathologic specimen shows lesion consisting of predominantly lepidic tumour growth with foci of invasive acinar components of less than 5 mm in thickness (black arrow) (Hematoxylin-eosin stain; original magnification, ×100)

(30.0%) (Figs. 1, 2, 3 and 4). The 148 patients included 54 (36.5%) men and 94 (63.5%) women, with age ranging from 26 to 78 years (mean age 53.55 years ± 8.87 years). Of the 148 patients, 91 had no symptoms, 16 complained of chest pain, 22 had a cough, nine had cough and shortness of breath, and ten patients presented with shortness of breath. Thirty nine of the 148 patients were smokers.

CT Features among different histopathologic Subtypes

There were statistically significant differences among histopathologic subtypes in terms of lesion size, vessel changes, and tumour-lung interface ($P < 0.05$) (Table 1). Of the 150 lesions,

mean pGGN size was (8.0 ± 1.6) mm ranging from 4.0 mm to 10.0 mm. The lesion size differed significantly between AAH and AIS, AAH and MIA, AAH and IPA ($P < 0.05$). The vessel changes occurred in 12.0% of AAH, 26.2% of AIS, 39.5% of MIA and 53.3% of IPA. Vessel changes differed significantly between AAH and MIA, AAH and IPA, AIS and IPA ($P < 0.05$) (Fig. 5). Lesions with clear tumour-lung interface were 48.0% of AAH, 69.0% of AIS, 84.2% of MIA, and 86.7% of IPA. Tumour-lung interface differed significantly between AAH and MIA, AAH and IPA, AIS and IPA ($P < 0.05$) (Figs. 1, 2, 3 and 4). There were no statistically significant differences among histopathologic subtypes in terms of density, bubble-like sign, air-bronchogram, and margin ($P > 0.05$).

Fig. 4 CT and histopathologic photomicrograph of IPA **a**. Thin-section CT image shows a pGGN located in the apical posterior segment of the left upper lobe (white arrow) with diameter of 9 mm, and clear tumour-lung interface; **b**. Photomicrograph of histopathologic specimen shows

neoplastic cells lining preexisting alveolar structures with invasive component measuring larger than 5 mm (black arrow) (Hematoxylin-eosin stain; original magnification, ×100).

Table 1 CT features in different histopathologic subtypes

CT Features		Histopathologic Subtypes				P value
		AAH	AIS	MIA	IPA	
Number of pGGNs		25 (16.7)	42 (28.0)	38 (25.3)	45 (30.0)	
Size (± SD, mm) *		7.0±2.0	8.0±1.5	8.3±1.2	8.4±1.7	0.020
Density (± SD, HU) *		−541.6±125.0	−506.2±151.5	−488.3±112.2	−487.3±142.0	0.325
Bubble-like sign		8 (32.0)	11 (26.2)	15 (39.5)	12 (26.7)	0.544
Air bronchogram		6 (24.0)	15 (35.7)	9 (23.7)	13 (28.9)	0.626
Vessel changes		3 (12.0)	11 (26.2)	15 (39.5)	24 (53.3)	0.003
Margin	Smooth	15 (60.0)	22 (52.4)	11 (28.9)	16 (35.6)	0.085
	Lobular	4 (16.0)	12 (28.6)	14 (36.8)	10 (22.2)	
	Spiculated	5 (20.0)	6 (14.3)	6 (15.8)	10 (22.2)	
	Lobular+Spiculated	1 (4.0)	2 (4.8)	7 (18.4)	9 (20.0)	
Clear tumour-lung interface		12 (48.0)	29 (69.0)	32 (84.2)	39 (86.7)	0.002

pGGN=Pure ground-glass nodule; AAH=Atypical adenomatous hyperplasia; AIS=Adenocarcinoma in situ; MIA=Minimally invasive adenocarcinoma; IPA= Invasive pulmonary adenocarcinoma; HU=Hounsfield unit; SD=Standard deviation. Except where indicated, data are the number (%) of nodules. * Data are means±standard deviation

CT features in preinvasive and invasive groups

Of the 150 lung adenocarcinomas, 67 (44.7%) were preinvasive, while 83 (55.3%) were invasive. In univariate logistic regression analysis, there were differences between preinvasive and invasive groups in terms of the vessel changes (area under ROC curve (AUC), 0.630; sensitivity, 47.0%; specificity, 79.1%), margin (AUC, 0.641; sensitivity, 67.5%; specificity, 55.2%), and tumour-lung interface (AUC, 0.622; sensitivity, 85.5%; specificity, 38.8%) ($P < 0.05$). The vessel changes were demonstrated in 20.9% of preinvasive lesions and 47.0% of invasive lesions. The preinvasive lesions with smooth margin were up to 55.2%, while invasive lesions with smooth margin were about 32.5%. Lesions with clear tumour-lung interface were 61.2% of preinvasive lesions and 85.5% of invasive lesions. Lesion size, density, bubble-like sign, and air-bronchogram were not significantly different between the

two groups ($P > 0.05$) (Table 2). Multivariate logistic regression analysis showed that the vessel changes, unsmooth margin and clear tumour-lung interface were significant predictive factors for lesion invasiveness. Odds ratio (OR) for vessel changes, margin, and tumour-lung interface were 2.57 (95% CI 1.17-5.62; $P=0.018$), 1.83 (95% CI 1.25-2.68; $P=0.002$), and 4.25 (95% CI 1.78-10.14; $P=0.001$), respectively.

Discussion

According to the 2011 IASLC/ATS/ERS and 2015 World Health Organization lung adenocarcinoma classification [4, 14, 15], AIS and MIA have a 100% 5-year disease-free survival [16, 17]. So determining the invasiveness of pGGN becomes very important. Despite the overlapping CT characteristics of different histopathologic subtypes, we found that the
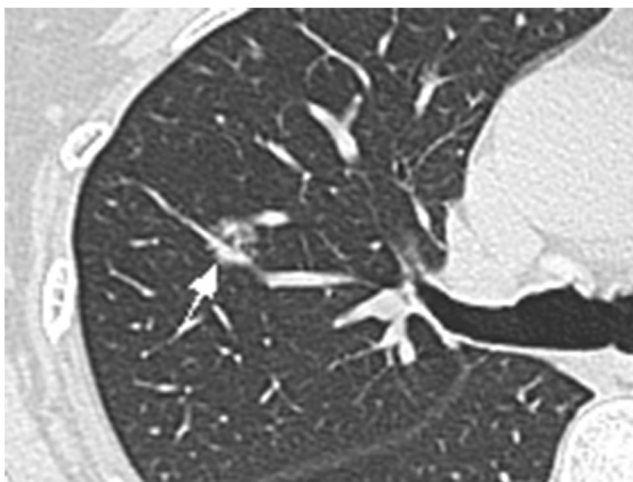
Fig. 5 Illustration of an invasive pulmonary adenocarcinoma (IPA) Note the presence of a dilated vessel within the pure ground-glass nodule (white arrow)

Table 2 CT features between the two histopathologic groups

CT Features		Histopathologic Groups		P value
		Preinvasive	Invasive	
Number of pGGNs		67 (44.7)	83 (55.3)	
Size (± SD, mm) *		7.6±1.7	8.4±1.5	0.269
Density (± SD, HU) *		−519.4±142.3	−487.8±128.5	0.472
Bubble-like sign		19 (28.4)	27 (32.5)	0.582
Air bronchogram		21 (31.3)	22 (26.5)	0.515
Vessel changes		14 (20.9)	39 (47.0)	0.001
Margin	Smooth	37 (55.2)	27 (32.5)	0.010
	Lobular	16 (23.9)	24 (28.9)	
	Spiculated	11 (16.4)	16 (19.3)	
	Lobular+Spiculated	3 (4.5)	16 (19.3)	
Clear tumour-lung interface		41 (61.2)	71 (85.5)	0.001

occurrence rate of vessel changes and clear tumour-lung interface tended to increase from AAH to IPA. In addition, preinvasive pGGNs demonstrate more smooth margin.

There have been some reports regarding subcentimeter lung cancer in the literature [11, 12, 18, 19]. Imaging reports regarding pGGN ≤10 mm are very rare after the new classification. Kato et al. reported that 54.55% subcentimeter adenocarcinomas were invasive [18]. There has been no unified consensus on the indications for surgical resection in pGGNs, especially pGGNs ≤10 mm [20–22]. Previous studies showed the cut-off value of 10 mm for predicting invasive lesions, and the majority of pGGNs ≤10 mm were preinvasive lesions with a specificity of 100% [8, 9, 23]. However, pGGNs ≤10 mm also included MIA and IPA [10–13]. In our study, we found that 83 (55.3%) of the 150 lesions with pGGN ≤10 mm were invasive, including 45 (30.0%) IPAs. There were various prognosis in different histopathologic subtypes, which required accurate diagnosis even in subcentimeter lesions.

In a previous study, AAH size was commonly less than 5 mm [14]. However, in our study, mean AAH size was (7.0 ± 2.0) mm. A previous study showed that with the increase in invasiveness of lung adenocarcinoma with GGN, the lesion size increased accordingly [24]. We also found that the lesion size differed significantly between AAH and AIS, AAH and MIA, AAH and IPA, which indicate that benign lesions were relatively smaller than malignant lesions. The nodules included in this study were small in size, and the size differences among the four histopathologic subtypes were also too small. So the lesion size was not a reliable CT sign for indicating histopathologic subtypes. According to the 2013 Fleischner guidelines [21], solitary pGGNs ≤5 mm required no CT follow-up. However, in our previous study [25], we found that three pGGNs ≤5 mm increased in size or appeared solid component during the follow-up.

The CT characteristics of preinvasive and invasive GGNs were reported in previous studies [5–8, 26]. Gao et al. categorized the GGN-vessel relationships into four types and found they could help to distinguish malignant or invasive lesions from benign or preinvasive lesions [27]. Differing from Gao's study which mixed GGNs and benign lesions were included, our study only included subcentimeter pGGN adenocarcinoma, we believed that type I and type II GGN-vessel relationships in Gao's study were normal conditions and vessel changes within the GGN were earlier and more accurate to reflect the histopathologic process. So the distorted/dilated vessel and vascular convergence within the pGGN were defined as vessel changes in this study, our results showed that the vessel changes were associated with lesion invasiveness, and the vessel changes occurred in 53.3% of IPA, while only occurring in 12.0% of AAH. We also found that there were significant differences among histopathologic subtypes in terms of margin and tumour-lung interface. The preinvasive

lesions manifested smoother margins (55.2%) than invasive lesions (32.5%). Invasive lesions often showed clear tumour-lung interface (85.5%). So the pGGN with clear tumour-lung interface and lobular with spiculated margin had a tendency for invasiveness; those were correlated with previous studies [20, 28, 29]. There were no significant differences among histopathologic subtypes in terms of CT attenuation, bubble-like sign and air bronchogram, and those might due to our study population in which the CT attenuation varied relatively small and occurrence rates of bubble-like sign and air bronchograms were relatively low.

The present study has several limitations. First, this study had patient selection bias, since only surgical resected pGGNs were enrolled, the CT characteristics of which could more likely be a malignancy. In addition, since the 2013 Fleischner guidelines were published, little change may have taken place in the management of the sub-solid nodules. Second, the size measurement of pGGNs ≤10 mm was sometimes difficult, especially with unclear tumour-lung interface lesions. Finally, the AUC, sensitivity and specificity values were not very high in general.

Conclusion

Invasive lesions are found in 55.3% of subcentimeter pGGNs in our cohort, the vessel changes within the lesion, unsmooth margin and clear tumour-lung interface may indicate the invasiveness of lung adenocarcinoma with pGGNs ≤10 mm in diameter.

References

1. Matsuguma H, Mori K, Nakahara R et al (2012) Characteristics of subsolid pulmonary nodules showing growth during follow-up with CT scanning. Chest 143:436–443

2. Chang B, Hwang JH, Choi YH et al (2013) Natural history of pure ground-glass opacity lung nodules detected by low-dose CT scan. Chest 143:172–178

3. Sawabata N, Kanzaki R, Sakamoto T et al (2014) Clinical predictor of pre- or minimally invasive pulmonary adenocarcinoma: possibility of sub-classification of clinical T1a. Eur J Cardiothorac Surg 45:256–261

4. Yoshizawa A, Motoi N, Riely GJ et al (2011) Impact of proposed IASLC/ATS/ERS classification of lung adenocarcinoma: prognostic subgroups and implications for further revision of staging based on analysis of 514 stage I cases. Mod Pathol 24:653–664

5. Lim HJ, Ahn S, Lee KS et al (2013) Persistent pure ground-glass opacity lung nodules ≥ 10 mm in diameter at CT scan: histopathologic comparisons and prognostic implications. Chest 144:1291–1299

6. Lee HJ, Jin MG, Chang HL et al (2009) Predictive CT findings of malignancy in ground-glass nodules on thin-section chest CT: the effects on radiologist performance. Eur Radiol 19:552–560

7. Jiang B, Wang J, Jia P et al (2013) The value of CT attenuation in distinguishing atypical adenomatous hyperplasia from adenocarcinoma in situ. Zhongguo Fei Ai Za Zhi 16:579–583

8. Lee SM, Park CM, Goo JM et al (2013) Invasive pulmonary adenocarcinomas versus preinvasive lesions appearing as ground-glass nodules: differentiation by using CT features. Radiology 268:265–273

9. Nakata M, Sawada S, Saeki H et al (2003) Prospective study of thoracoscopic limited resection for ground-glass opacity selected by computed tomography. Ann Thorac Surg 75:1601–1605

10. Asamura H, Suzuki K, Watanabe S et al (2003) A clinico-pathological study of resected subcentimeter lung cancers: a favorable prognosis for ground glass opacity lesions. Ann Thorac Surg 76:1016–1022

11. Zhou Q, Suzuki K, Anami Y et al (2009) Clinicopathologic features in resected subcentimeter lung cancer–status of lymph node metastases. Interact Cardiovasc Thorac Surg 10:53–57

12. Sakurai H, Nakagawa K, Watanabe SI et al (2015) Clinicopathologic features of resected subcentimeter lung cancer. Ann Thorac Surg 99:1731–1738

13. Mao H, Labh K, Han F et al (2015) Diagnosis of the invasiveness of lung adenocarcinoma manifesting as ground glass opacities on high-resolution computed tomography. Thorac Cancer 7:129–135

14. Travis WD, Brambilla E, Noguchi M et al (2011) International Association for the Study of Lung Cancer/American Thoracic Society/European Respiratory Society: international

multidisciplinary classification of lung adenocarcinoma: executive summary. Proc Am Thorac Soc 8:381–385

15. Travis WD, Brambilla E, Nicholson AG et al (2015) The 2015 world health organization classification of lung tumors: impact of genetic, clinical and radiologic advances since the 2004 classification. J Thorac Oncol 10:1243–1260

16. Liao JH, Amin VB, Kadoch MA et al (2014) Subsolid pulmonary nodules: CT–pathologic correlation using the 2011 IASLC/ATS/ERS classification. Clin Imaging 39:344–351

17. Yip R, Wolf A, Tam K et al (2016) Outcomes of lung cancers manifesting as nonsolid nodules. Lung Cancer 97:35–42

18. Kato F, Hamasaki M, Miyake Y et al (2012) Clinicopathological characteristics of subcentimeter adenocarcinomas of the lung. Lung Cancer 77:495–500

19. Hamatake D, Yoshida Y, Miyahara S et al (2012) Surgical outcomes of lung cancer measuring less than 1 cm in diameter. Interact Cardiovasc Thorac Surg 15:854–858

20. Lee HY, Choi YL, Lee KS et al (2014) Pure ground-glass opacity neoplastic lung nodules: histopathology, imaging, and management. AJR 202:224–233

21. Naidich DP, Bankier AA, Macmahon H et al (2013) Recommendations for the management of subsolid pulmonary nodules detected at CT: a statement from the fleischner society. Radiology 266(1):304–317

22. Sim HJ, Choi SH, Chae EJ et al (2014) Surgical management of pulmonary adenocarcinoma presenting as a pure ground-glass nodule. Eur J Cardiothorac Surg 46:632–636

23. Jin X, Zhao SH, Gao J et al (2015) CT characteristics and pathological implications of early stage (T1N0M0) lung adenocarcinoma with pure ground-glass opacity. Eur Radiol 25:2532–2540

24. Jones KD (2013) Whence lepidic?: the history of a Canadian neologism. Arch Pathol Lab Med 137:1822–1824

25. Wu F, Cai ZL, Tian SP et al (2016) Value of baseline clinical and CT characteristics for predicting the progression of persistent pure ground-glass nodule 10 mm or less in diameter. Acta Academiae Medicinae Sinicae 38(4):371–377

26. Honda T, Kondo T, Murakami S et al (2013) Radiographic and pathological analysis of small lung adenocarcinoma using the new IASLC classification. Clin Radiol 68:21–26

27. Gao F, Li M, Ge X et al (2013) Multi-detector spiral CT study of the relationships between pulmonary ground-glass nodules and blood vessels. Eur Radiol 23:3271–3277

28. Fan L, Liu SY, Li QC et al (2011) Pulmonary malignant focal ground-glass opacity nodules and solid nodules of 3 cm or less: comparison of multi-detector CT features. Eur Radiol 55:279–285

29. Si MJ, Tao XF, Du GY et al (2016) Thin-section computed tomography-histopathologic comparisons of pulmonary focal interstitial fibrosis, atypical adenomatous hyperplasia, adenocarcinoma in situ, and minimally invasive adenocarcinoma with pure ground-glass opacity. Eur Radiol 85:1708–1715